

# International Conference on Space Optics—ICSO 2014

La Caleta, Tenerife, Canary Islands

7–10 October 2014

*Edited by Zoran Sodnik, Bruno Cugny, and Nikos Karafolas*



## ***Direct hot slumping of thin glass foils for future generation x-ray telescopes: current state of the art and future outlooks***

*B. Salmaso*

*S. Basso*

*C. Brizzolari*

*M. Civitani*

*et al.*



## DIRECT HOT SLUMPING OF THIN GLASS FOILS FOR FUTURE GENERATION X-RAY TELESCOPES: CURRENT STATE OF THE ART AND FUTURE OUTLOOKS

B. Salmaso<sup>1,2</sup>, S. Basso<sup>1</sup>, C. Brizzolari<sup>1,3</sup>, M. Civitani<sup>1</sup>, M. Ghigo<sup>1</sup>, G. Pareschi<sup>1</sup>, D. Spiga<sup>1</sup>, G. Tagliaferri<sup>1</sup>, G. Vecchi<sup>1</sup>

<sup>1</sup>INAF/Brera Astronomical Observatory, Via E. Bianchi 46, 23807 Merate, Italy

<sup>2</sup>Università degli Studi dell'Insubria, Via Valleggio 11, 22100 Como, Italy

<sup>3</sup>Università di Milano-Bicocca, piazza della Scienza 3, 20126 Milano, Italy

### ABSTRACT

To significantly improve the performances of the current X-ray observatories, the next generation of X-ray telescopes has to be characterized by a large effective area ( $A_{\text{eff}} \sim 2 \text{ m}^2$  at 1 keV) and angular resolution better than 5 arcsec. The large dimension implied by these requirements forces the use of a modular approach, splitting the optics into segments. Moreover, lightweight materials, such as glass, have to be selected for the segmented optics in order to maintain a manageable weight for the optics. Since 2009 we are developing a direct hot slumping technique assisted by pressure, in which the glass optical surface is in contact with the mould and a pressure is applied in order to force the glass to copy the mould shape. A cold slumping step is used then to integrate the mirror segments into the final Wolter-I configuration. We present the state of the art of our hot slumping technology, comparing the results obtained with different glass types and mould materials. We also provide an overview of the possibilities of this technology also in view of future developments.

### I. INTRODUCTION

Unlike normal incidence reflective optics, reflective optical elements for X-rays are designed to reflect at shallow incident angles. In this configuration, the collecting area is a small fraction of the geometric area; therefore several mirrors have to be nested to increase the effective area of the telescope, so that the optical modules dominate the mass budget of the instrument payload.

Future generation X-ray telescopes, like ATHENA [1], need to be realized with lightweight optics providing both large effective area ( $A_{\text{eff}} = 2 \text{ m}^2$  at 1 keV) and high angular resolution (5 arcsec HEW, Half Energy Width). Materials lighter than Nickel (as used for XMM) or thick Zerodur glass (as used for Chandra) are therefore to be considered as candidates for lightweight, high-performances optics. A new technology, different from the replica process of the XMM Nickel shells or the direct polishing of the Chandra thick glasses, has to be developed. The Brera Astronomical Observatory (INAF-OAB) is developing the Slumped Glass Optics (SGO) technology to manufacture the modular elements required for the optics of the ATHENA mission. In our laboratories we form thin glasses (0.4 mm thin) by direct hot slumping, assisted by pressure, replicating the shape of a cylindrical mould. The formed foils are then stacked into Wolter-I configuration via a dedicated Integration Machine (IMA), to form the X-ray Optical Unit (XOU), the basic element of the telescope.

### II. SLUMPED GLASS OPTICS TECHNOLOGY

The SGO technology is based on thin glasses curved by hot slumping with a replica process and then integrated in the Wolter I configuration on a dedicated equipment. We are working on this technology since 2009. The research was supported until June 2013 by the European Space Agency (ESA) and proceeded with the collaboration of several institutes and Italian companies: Max Planck Institut für Extraterrestrische Physik (MPE, Garching, Germany), BCV-Progetti (Milano, Italy), ADS-International (Lecco, Italy), and Media Lario Technologies (Bosisio Parini, Italy). The study is still pursued to optimize our SGO technology.

Each individual glass of the XOU has to be curved in a furnace with a proper thermal cycle fit to enable a good surface roughness and the optimal curvature. In our laboratories we have developed a slumping process assisted by pressure [2], whose setup has been patented (TO2013A000687, 12/08/2013). In Fig 1 we show the furnace, the slumping mould, the glass and the muffle to enable the pressure application. The glass, slumped to a size larger than the mould, also acts as a membrane to divide the muffle chamber in two parts: the bottom part has a lower pressure, which drags the glass toward the mould surface and forces it into contact. The slumped glass has then to be trimmed to the final dimension, 200 x 200 mm. The typical thickness of the glass is 0.4 mm.

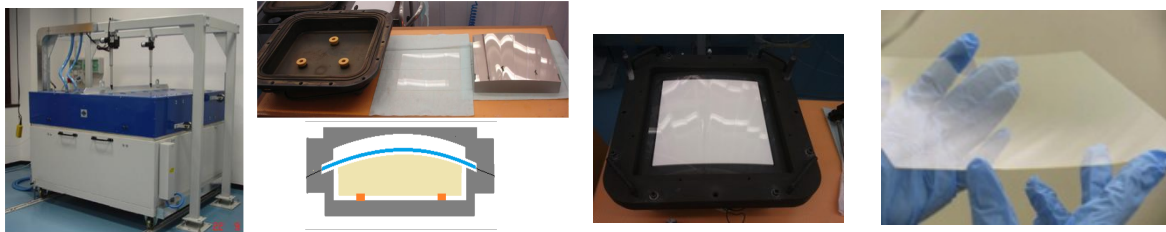


**Fig. 1.** From left: the furnace at our laboratories; the muffle, the glass, the slumping mould and the slumping set up; the slumped glass after the trimming.

The slumped glasses are characterized in shape with a Long Trace Profilometer for 1-D profiles and with the Characterization Universal Profilometer (CUP), developed at our laboratories, for 2-D maps [3]. Moreover, their surface roughness is characterized with an Atomic Force Microscope (AFM), a WYKO Phase Shift Interferometer and a Micro-Finish Topographer (MFT) [4].

The slumped glasses have cylindrical shape and they have to be integrated into the final Wolter-I configuration. We obtain this step via an ad-hoc designed and developed machine named Integration Machine (IMA) (Fig.2). The glasses are stacked and glued with glass ribs which, in addition to keep the mirror aperture clear by a proper spacing, endow the structure with mechanical stiffness, and eventually freeze into the glasses the Wolter-I profiles of the integration mould, thus correcting for residual low frequency error profiles [5]. Finite Element Analysis was performed with the ANSYS software [6] to evaluate the capability of the process to correct the initial errors at different spatial wavelengths: the basic result is that long-period errors are corrected almost entirely, whereas errors over a few cm scale remain almost unchanged after the integration.

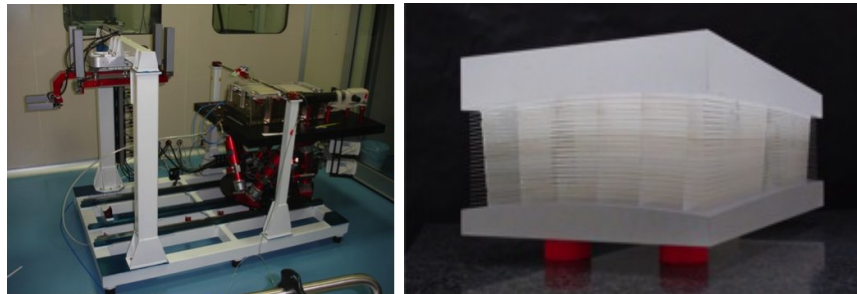


**Fig. 2.** Left: the Integration Machine. Right: XOU made of glasses stacked with reinforcing ribs.

An opto-mechanical study for different types of materials and different XOU design was recently performed fulfilling the requirements specified by the ATHENA mission [7]. The study, already performed for the IXO [6] X-ray telescope with a 20 m focal length and an effective area of 3 m<sup>2</sup> at 1 keV, was reviewed for a 12 m focal length telescope, with 2 m<sup>2</sup> effective area at 1 keV, the characteristics of ATHENA. In Fig. 3 we show a possible distribution of the XOUs inside the optical module structure.

Ring	N° XOU	N° ribs/shell
1	8	6
2	16	4
3	16	6
4	24	5
5	24	6
6	32	5
7	32	6

**Fig. 3.** Overview of the spokes wheel concept and XOUs repartition.

### III. STATE-OF-THE-ART PERFORMANCES

The first prototype of SGO, the Proof of Concept #1 (PoC#1), was produced using 0.4 mm thick Schott D263 glass foils, slumped on a Pt-coated Fused Silica cylindrical mould [8]. The resulting Half Energy Width (HEW) was 80 arcsec, affected by a high surface roughness, because of the utilization of a metal membrane for pressure application and poorly shaped integration moulds in Metapore, a material difficult to figure precisely.

The subsequent prototype, XOUBB (X-Ray Optical Unit Bread Board) was then realized with D263 glass foils slumped on moulds of different materials and using different settings for the application of pressure [2]. Its main goal was to manufacture a complete optical unit model of the IXO optical system, demonstrating in particular the capability of stacking of plate pairs with the IMA.

A later prototype (PoC#2) was produced with Schott AF32 glasses slumped on a Zerodur K20 mould; a better matching of the Coefficient of Thermal Expansion (CTE) of the two materials has enabled smaller errors in the slumped glass shape. The glasses were then integrated using newly procured BK7 integration moulds, with much more accurate Wolter-I profiles with respect to the previous Metapore moulds. These modifications have allowed the complete module to reach a HEW of  $\sim 22$  arcsec and the better plate pair a HEW of  $\sim 20$  arcsec, directly measured in-focus at 0.27 keV at the PANTER facility [9].

Finally, a last prototype (PoC#3) was realized with Corning Eagle glass foils slumped on a newly procured Zerodur K20 slumping mould, with better surface roughness with respect to the previous one [10]. Despite the overall HEW higher with respect to the PoC#2, the X-ray analysis, performed at the PANTER/MPE facility in pencil beam mode, showed a best HEW value, in a portion of the module, of 5.5 arcsec at 0.27 keV (Fig. 4) [9]. Moreover, the impact of the roughness in the 0.27-1.49 keV range was considerably reduced with respect to the previous prototypes, denoting a better surface roughness.

Table 1: Description of the prototypal models realized @ INAF-OAB

	PoC#1	XOU-BB	PoC#2	PoC#3
N° plate pairs	2	3+17	3+1	1
Configuration	parallel	parallel	Cofocal	Not applicable
Slumped glass material	D263	D263	AF32	Eagle
Slumping mould material	Fused Silica with Pt coating	Various	Zerodur K20	Zerodur K20
Setup for pressure application (slumping)	Metal membrane	Various	Glass	Glass
Integration moulds material	Metapore	Metapore	BK7	BK7
Integration moulds profile accuracy (equivalent HEW)	40 arcsec	40 arcsec	8 arcsec	8 arcsec
Backplane & ribs material	BK7	BK7	BK7	Borofloat
Measured angular resolution of the prototype (HEW)	80 arcsec	60 arcsec	22 arcsec	30 arcsec
Best of the module	Not available	48 arcsec	20.1	5.5arcsec

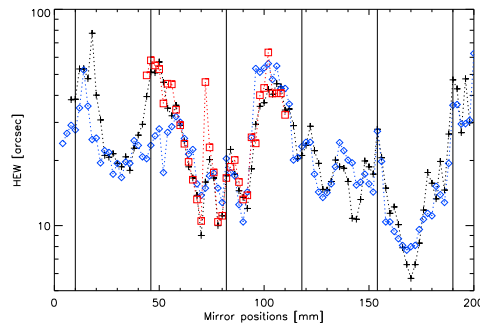


Fig. 4. The PoC#3 calibration at PANTER/MPE, obtained via with pencil beam characterization measurements @ 0.27 keV (black), @ 0.93 keV (red), and @ 1.49 keV (blue). The black, solid lines indicate the rib positions.

The detailed results for the last two prototypes can be found elsewhere [9]: this paper concentrates on presenting the currently achieved know-how and performance of the hot slumping technology @ INAF-OAB.

#### IV. THE DIRECT HOT SLUMPING ASSISTED BY PRESSURE

The hot slumping is a replica process in which the temperature is brought high enough to soften the glass and slump it over the mould; when the glass is brought back to room temperature, it retrieves its solid state and thereby copies the mould profile. If the surface of the glass in contact with the mould is the optical one (direct approach) the roughness of the mould surface is replicated on the glass side, at least partially. On the other hand, if the surface in contact with the mould is the non-optical one (indirect approach), all the glass thickness variations are transferred to the optical surface. In both cases, the quality of the X-ray telescope is degraded and those effects have to be minimized.

Different glass types can be used. Schott D263 glasses were used for instance at the NASA-Goddard laboratories and Columbia University (USA) for the NuSTAR optics [11]; they were also used in an early phase of our research [8] and are still currently used in the Max Planck Institut für Extraterrestrische Physik (MPE, Germany) [12]. The Schott AF32 glass type was then used in our laboratories. More recently, the Corning Eagle XG glass was used, as Schott discontinued the production of the AF32 glass in the size necessary for our setup. A mould in Zerodur K20 was selected, as it does not require an anti-sticking layer (unlike Fused silica, Silicon

or Silicon Carbide).

The good coupling of the CTE of the glass and the mould is a key factor for the optical quality of the slumped glass ( $CTE_{K20} = 2.0 \cdot 10^{-6}/^{\circ}K$ ,  $CTE_{D263} = 7.2 \cdot 10^{-6}/^{\circ}K$ ,  $CTE_{AF32} = 3.2 \cdot 10^{-6}/^{\circ}K$ ,  $CTE_{Eagle} = 3.17 \cdot 10^{-6}/^{\circ}K$ ), as it avoids the shear of the optical surface on the mould when the temperature is decreased, thereby reducing errors in the centimeter spatial wavelengths. These types of errors are expected to be present on the glass surface, when the glass is in contact with the mould [13], and they have to be minimized as, unlike low frequency errors, they are not corrected by the integration procedure.

Another key factor is the applied pressure, that helps reducing the mid frequency errors. The resulting CUP maps of two glasses slumped with pressure of  $50 \text{ g/cm}^2$  and  $20 \text{ g/cm}^2$  are compared in Fig 5: the higher mid frequency errors content is evident in the glass slumped with lower pressure (Fig. 5, right).

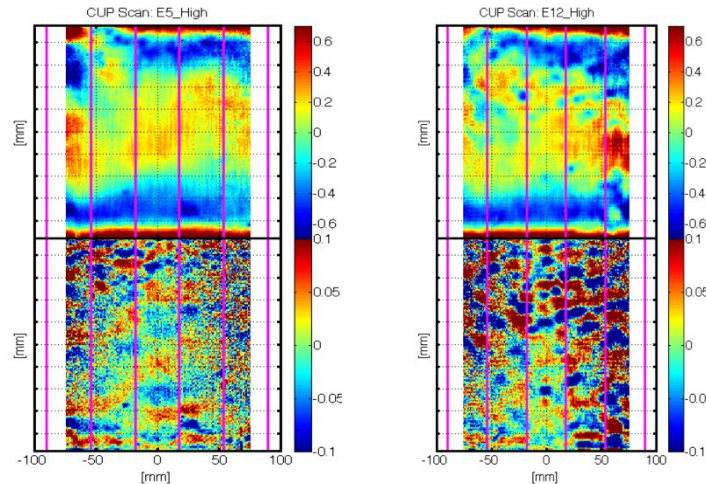


**Fig. 5.** The effect of pressure application during the slumping: on the left the CUP map for an Eagle glass slumped with  $P = 50 \text{ g/cm}^2$ , on the right for an Eagle glass slumped with  $P = 20 \text{ g/cm}^2$ . The maps show the residuals after the subtraction of Legendre polynomial up to the 2<sup>th</sup> order on the top, while on the bottom the residuals after the removal of the 8<sup>th</sup> order. These figures clearly show that the content of errors in the cm range decreases with the applied pressure.

Actually, a trade-off for the pressure value has to be found, as higher pressure values reduce the mid-frequencies but at the same time increase the high frequency errors. The Zerodur K20 surface is in fact crowded with peaks that degrade the glass surface in contact with the mould [14]. As the surface roughness of the K20 mould used for the production of the PoC#2 was degraded after several slumping cycles, a new Zerodur K20 mould was purchased (named hereafter MK20-20). Improved surface roughness of the slumped glasses was obtained with this mould [10]. Still the pressure value could not be set higher than the standard  $50 \text{ g/cm}^2$ , in order to not degrade the slumped glass surface. In Fig. 6, the roughness of a Eagle glass, slumped with direct approach at pressure of  $50 \text{ g/cm}^2$  (blue lines), is compared with the roughness of the MK20-20 slumping mould (red/orange lines). It appears that, in the  $0.1\text{-}100 \mu\text{m}$  spatial wavelength region, the roughness of the mould is only slightly replicated on the glass optical surface. In contrast, in the mm range, the roughness of the glass is comparable to the one of the mould.

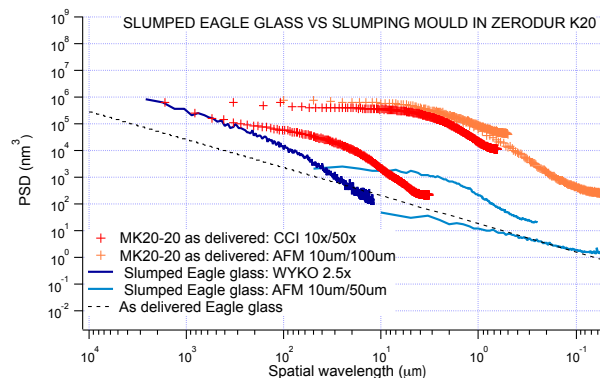


**Fig. 6.** PSD comparison of the MK20-20 and an Eagle slumped glass. This graph shows that, in the high frequency region, the roughness is only slightly replicated on the slumped glass foils.



In Fig. 6 we also traced the PSD of the Eagle glass before being formed. In order to avoid HEW degradation at energies higher than 1 keV and up to 5 keV, we should aim at preserving the roughness of the glass optical surface as closer as possible to that PSD, which will represent our target value for the surface roughness, especially in the mm range. In section V we outline the work ongoing for the indirect slumping, both on Zerodur K20 and Silicon Nitride as slumping moulds, aiming at preserving the native glass roughness for the optical glass surface.

Finally, we show the CUP maps obtained on two glasses slumped on the new MK20-20 (Fig. 7). The E16 was one of the two glasses integrated in the PoC#3. It was slumped on MK20-20 after two preliminary slumping cycles that suffered from air entrapping in the central region and most likely asymmetric deformation of the K20 material [10]. Therefore, this glass shows residual errors in the central region (Fig.7 left/bottom) that degrade the resulting HEW (Fig.4). To investigate the K20 deformation on subsequent slumping cycles, other glasses were slumped on the same mould with the same process parameters. The glass, shown in the right side of Fig. 7, was slumped after 5 slumping cycles, giving better results in terms of mid frequency errors. It was also slumped with a prolonged soaking time, thus affecting the surface roughness. An optimal value needs to be found also for the soaking time.

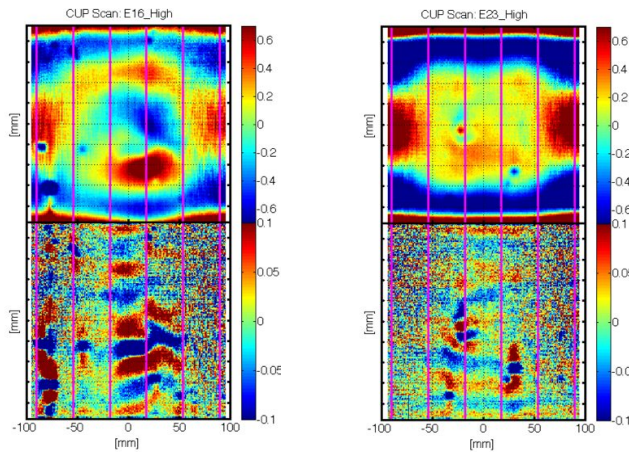


**Fig. 7.** The effect of K20 stabilization of its deformations together with the effect of increasing the soaking time: on the left the CUP map for an Eagle glass slumped on a K20 mould not yet stabilized, on the right for an Eagle glass slumped after several slumping cycles and with an increased soaking time. The maps show the residuals after the subtraction of Legendre polynomial up to the 2<sup>th</sup> order on the top, while on the bottom the residuals after the removal of the 8<sup>th</sup> order

Regarding the deformation of the K20 material, Silicon Nitride is considered a very promising alternative material, because it does not exhibit deformation after a slumping cycle with pressure (see section V).

## V. RECENT PROGRESS OF SGO

After demonstrating the capabilities of the SGO technology for high-resolution X-ray space telescopes, we considered the possibility to improve the performances bypassing the limits of our setup. Namely, two limits were considered key factors: the Zerodur K20 deformation and the degradation of the optical surface on the direct slumping.

The research on the Silicon Nitride, as a material for the slumping moulds, was driven by three key points: a higher rigidity with respect to the Zerodur K20 (Young's Modulus for Si<sub>3</sub>N<sub>4</sub> = 300 GPa, for K20 = 84.7 GPa), a better matching of the CTE with the one of the glass (CTE<sub>Si<sub>3</sub>N<sub>4</sub></sub> = 3.4×10<sup>-6</sup>/°K, CTE<sub>Eagle</sub> = 3.17 10<sup>-6</sup>/°K), and a higher thermal conductivity (k) with respect to the Zerodur K20 (k<sub>Si<sub>3</sub>N<sub>4</sub></sub> = 33 W/mK, k<sub>K20</sub> = 1.63 W/mK). We hence have purchased flat sample moulds of Silicon Nitride. Several slumping tests, with increasing temperature and pressure, were performed on a sample to ascertain the absence of sticking. No sticking ever occurred, proving this material as a good candidate for the slumping technique.



**Fig. 8.** The setup for the slumping of Eagle glasses on Si<sub>3</sub>N<sub>4</sub> sample mould: the glass was cut to circular shape with diameter suitable for the application of pressure.

Moreover, the increased rigidity of the  $\text{Si}_3\text{N}_4$  with respect to the Zerodur K20 was shown by performing profiles measurements on the  $\text{Si}_3\text{N}_4$  diameter before and after the slumping with standard process parameters (Fig. 9). No deformation occurred on  $\text{Si}_3\text{N}_4$ , whilst we experienced it on Zerodur K20 mould. The rigidity of this material makes also possible to produce a cylindrical slumping mould thinner than the mould in K20, thus reducing the cost of the mould production: FEA showed that a negligible deformation for a cylindrical mould with dimension 250 x 250 mm and radius of curvature of 1 m, in our working conditions, can be obtained with mould thickness of 50 mm for the K20 whilst 32 mm for the  $\text{Si}_3\text{N}_4$ .

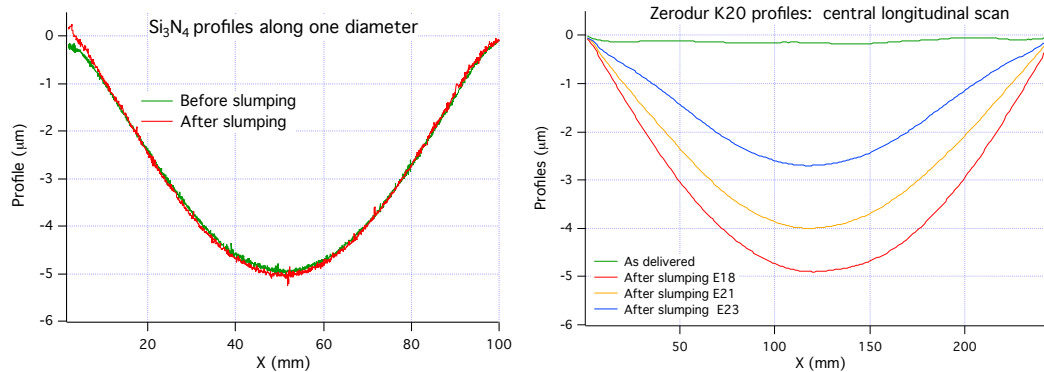


**Fig. 9.** Shape stability of  $\text{Si}_3\text{N}_4$  compared to the deformation of the Zerodur K20: on the left, the  $\text{Si}_3\text{N}_4$  profiles along one diameter, as measured with the Zeiss contact profilometer before and after the slumping; on the right, the K20 profiles along the central longitudinal scan, as measured with the LTP after several slumping cycles.

From the roughness point of view, the Silicon Nitride sample moulds were very rough, with  $\text{rms@WYKO} = 207 \text{ \AA}$  (Fig. 11), as no special attention was paid to the polishing of the mould in this first phase of the research. The surface was crowded with peaks (Fig. 10.c) and this entails a very poor quality of the slumped glass surface in contact with the mould (Fig.10-a). Still, the slumped glass surface not in contact with the mould (indirect approach) is almost comparable to the pristine glass (Fig.10-b). In Fig. 11, the roughness of the  $\text{Si}_3\text{N}_4$  slumping mould, and the ones of the slumped Eagle glass, considering both direct and indirect approaches are compared. The polishing capability on the  $\text{Si}_3\text{N}_4$  will be investigated in a later phase.

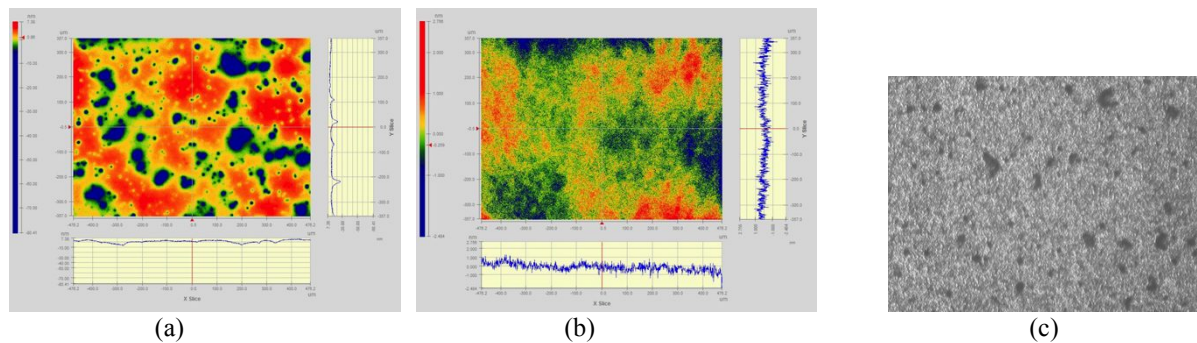


**Fig. 10.** Surface maps of an Eagle glass slumped on  $\text{Si}_3\text{N}_4$  mould (a and b) compared to the  $\text{Si}_3\text{N}_4$  mould surface (c). a) a MFT image of the slumped Eagle glass on the surface in contact with the mould,  $\text{rms} = 4.1 \text{ nm}$ ,  $\text{PV} = 87.8 \text{ nm}$  b) a MFT image of the slumped Eagle glass on the surface NOT in contact with the mould,  $\text{rms} = 0.5 \text{ nm}$ ,  $\text{PV} = 5.3 \text{ nm}$  c) an image of the  $\text{Si}_3\text{N}_4$  surface, taken with the Nomarski microscope with approximately the same field of view of the MFT images ( $\sim 1 \text{ mm}$ )

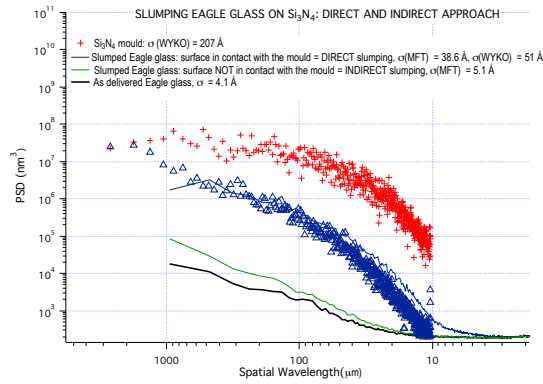


**Fig. 11.** PSD comparison of the  $\text{Si}_3\text{N}_4$  mould and an Eagle slumped glass. Red curve: the  $\text{Si}_3\text{N}_4$  mould measured with the WYKO. Blue curves: the slumped glass, surface in contact with the mould, measured both with the WYKO and the MFT. Green: the slumped glass, surface NOT in contact with the mould, measured with the MFT. Black: un-slumped glass, measured with the MFT. The PSD are computed as average of 5 measurements. Solid lines are from MFT, lines with markers are from WYKO.

We also started tests on the indirect slumping by using a mould in Zerodur K20 with concave cylindrical shape and a 2 m radius of curvature. Despite the low quality of the mould surface, we consider this a good test to check our setup with pressure application on cylindrical moulds also for the indirect slumping. Fig. 12.c shows the patterns present on the mould surface reproduced on the optical side of the slumped D263 glass, proving that the setup was correctly driving the glass in contact with the mould. The process parameters were the same as for the direct approach and yielded a longitudinal PV of about 40  $\mu\text{m}$ , to be compared with the 8  $\mu\text{m}$  longitudinal error of the slumping mould.

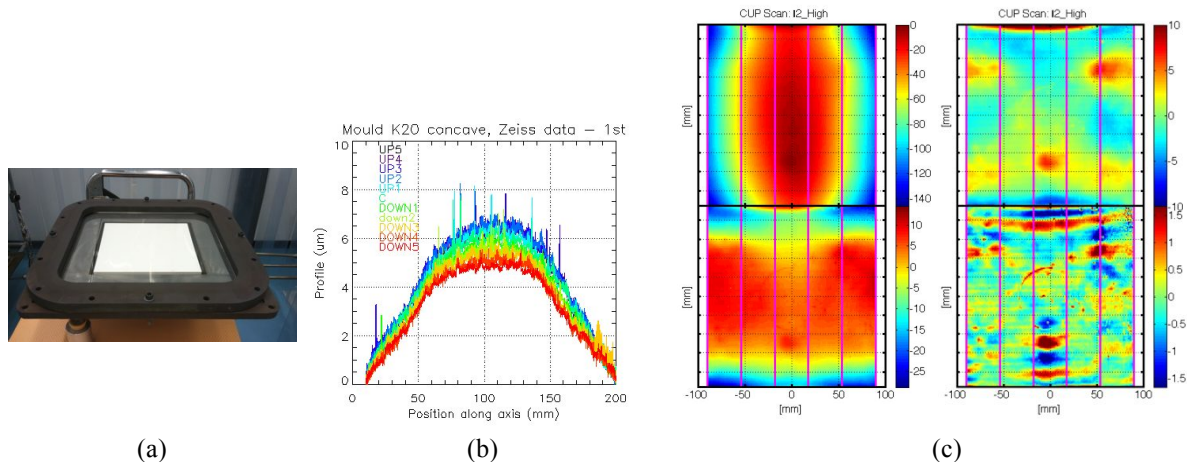


**Fig. 12.** Indirect slumping results. a) the setup for the indirect slumping, b) the longitudinal mould profiles as measured with the Zeiss contact profilometer, c) the CUP metrological characterization of the optical side of the slumped glass. The CUP data show in the first column the residual with respect to a theoretical cylinder with radius of curvature of 2 m (up) and a patch of the longitudinal scans (down), in the second column the same map after the subtraction of the 4<sup>th</sup> (up) and 8<sup>th</sup> (down) order Legendre polynomial.

VI. CONCLUSION AND OUTLOOK

The SGO technology developed at INAF-OAB has considerably advanced since 2009. Several prototypes have been already realized proving that the hot slumping technology assisted by pressure and our integration concept are a key combination for the realization of lightweight X-ray telescopes of future generation. To date the best result, on the overall prototype, was obtained with AF32 glasses slumped on Zerodur K20 (PoC#2), returning 22 arcsec at 0.27 keV. Improvement on the roughness was obtained purchasing a new slumping mould in Zerodur K20 and the best region of the PoC#3 prototype (produced with Eagle glasses) was 5.5 arcsec at 0.27 keV, with an overall increment of 1 arcsec on all the prototype by increasing the energy to 1.49 keV.

We are now working on alternative solutions for the observed deformation of the Zerodur K20 mould and the still high roughness of the slumped glasses with the direct approach.  $\text{Si}_3\text{N}_4$  seems to be a promising material, as it does not stick to the glass at our slumping temperature and pressure, as Zerodur K20, but in addition it does



not deform with the slumping cycles, owing to its higher stiffness. We have performed preliminary slumping tests of Eagle glasses over a flat sample of  $\text{Si}_3\text{N}_4$  and the results show that, despite the very high roughness of the mould surface, the glass surface not in contact with the glass has roughness values comparable with the one of pristine glasses. We have proven, both with the flat  $\text{Si}_3\text{N}_4$  sample and with a concave Zerodur K20 mould, that our setup for pressure application is suitable also for the indirect approach. For the next steps, we will work in parallel with the direct and indirect approach.

A research on the hot slumping for normal incidence mirrors is also planned: a first prototype was already produced at our laboratories [15] combining the good optical performances achievable on optics produced by means of the hot slumping technique with the lightweight and stiffness of the foamed material in sandwich-like structures.

## REFERENCES

- [1] Nandra, K., Barcons, X., Barret, D., Fabian, A., den Herder, J.W., Piro, L., Watson, M., “*Athena: The Advanced Telescope for High Energy Astrophysics*”, Mission proposal, <http://www.the-athena-x-ray-observatory.eu>
- [2] Ghigo, M., Basso, S., Borsa, F., Bavdaz, M., Citterio, O., Civitani, M., et al., “*Development of high angular resolution x-ray telescopes based on slumped glass foils*”, Proc. SPIE 8443, 84430R (2012).
- [3] M. M. Civitani, M. Ghigo, O. Citterio, P. Conconi, D. Spiga, G. Pareschi, L. Proserpio, “*3D characterization of thin glass x-ray mirrors via optical profilometry*”, Proc. SPIE 7803, 78030L (2010)
- [4] Parks, R.E., “*MicroFinish Topographer: surface finish metrology for large and small optics*”, Proc. SPIE 8126, 81260D, (2011).
- [5] Civitani, M., Basso, S., Citterio, O., Conconi, P., Ghigo, G., Pareschi, et al., “*Accurate integration of segmented X-ray optics using interfacing ribs*”, Optical engineering 52, (9), 091809 (2013).
- [6] Parodi, G., Martelli, F., Basso, S., Citterio, O., Civitani, M., Conconi, P., et al., “*Design of the IXO optics based on thin glass plates connected by reinforcing ribs*”, Proc. SPIE 8147, 81470Q-1 (2011).
- [7] Basso, S., Buratti, E., Civitani, M.M., Pareschi, G., Salmaso, B., Spiga, D., Tagliaferri, G., Eder, J., “*A high resolution large x-ray mission based on thin glass: optomechanical design*”, Proc SPIE 9144, 91444C (2014).
- [8] Proserpio, L., Ghigo, M., Basso, S., Conconi, P., Citterio, O., Civitani, M., et al., “*Production of the IXO glass segmented mirrors by hot slumping with pressure assistance: tests and results*” Proc. SPIE 8147, 81470M (2011).
- [9] Civitani, M., Basso, S., Ghigo, G., Pareschi, G., Salmaso, B., Spiga, D., et al., “*X-ray Optical Units made of glass: achievements and perspectives*”, Proc. SPIE 9144, 914416 (2014).
- [10] Salmaso, B., Basso, S., Brizzolari, C., Civitani, M.M., Ghigo, M., Pareschi, G., et al., “*Production of thin glass mirrors by hot slumping for X-ray telescopes: present process and ongoing development*”, Proc SPIE 9151, 91512W (2014)
- [11] Koglin, J.E., An, H., Barrière, N., Brejnholt, N.F., Christensen, F.E., Craig, W.W., Hailey, C.J., et al., “*First results from the ground calibration of the NuSTAR flight optics*”, Proc. SPIE 8147, 81470J (2011).
- [12] Winter, A., Breunig, E., Burwitz, V., Friedrich, P., Hartner, G., et al., “*Light-weight glass mirror systems for future x-ray telescopes*”, Proc. SPIE 8861, 88610Q (2013).
- [13] Jimenez-Garate, M. A., Hailey, C. J., Craig, W. W., Christensen, F. E., “*Thermal forming of glass microsheets for x-ray telescope mirror segments*”, Applied Optics 42, 4 (2003).
- [14] Salmaso, B., Bianco, A., Citterio, O., Pareschi, G., Pariani, G., Proserpio, L., et al., “*Micro-roughness improvement of slumped glass foils for X-ray telescopes via dip coating*”, Proc. SPIE 8861-60, (2013).
- [15] Canestrari, R., Ghigo, M., Pareschi, G., Basso, S., Proserpio, L., “*Investigation of a novel slumping technique for the manufacturing of stiff and lightweight optical mirrors*”, Proc. SPIE 7018, 7018D (2008).